6ICEGE 6th International Conference on Earthquake Geotechnical Engineering
1-4 November 2015
Christchurch, New Zealand

Excess Pore Water Pressure Generation of Loose Silty Sand under Cyclic Loading

M. A. L. Baki[1], M. M. Rahman[2] and S. R. Lo[3]

ABSTRACT

Liquefaction, which may be experienced during earthquakes, blasting, wave loading or sudden static loading, may cause saturated sandy ground to a very soft liquid-like material and many structures upon it sink or tilt, leading to no more use. Under such loading, generation of excess pore water pressure reduces the effective stresses and liquefaction occurs when the effective stresses approach to zero. It remains a critical earthquake-induced hazard for civil infrastructure. For this study, a series of two-way nonsymmetrical cyclic triaxial tests had been carried out to examine generation of excess pore water pressure of Sydney sand with fines up to 15%. It has been found, for compared test-pairs, that equivalent granular state parameter essentially captures the effects of fines in generation of excess pore water pressure. The effect of loading reversal on generation of excess pore water pressure is also examined and discussed.

Introduction

It is well established that the main mechanism associated with the phenomenon of liquefaction is the generation of excess pore water pressure (pwp) under seismic loading conditions (Hazırbaba 2005; Xenaki and Athanasopoulos 2003). Earthquakes, blasting, wave loading, impacts, vibrations, and explosives, which may cause liquefaction of soil, can induce residual pwp in saturated soils. It has a significant effect on the shear strength, stability and settlement characteristics of cohesionless soil deposits (Belkhatir et al. 2014; Charlie et al. 2013; Wijewickreme and Sanin 2010). Under sufficient number of loading cycles, progressive generation of excess pwp reduces the effective stresses to zero or close to zero to cause cyclic liquefaction. Depending on the form of cyclic liquefaction either cyclic mobility or cyclic instability (Baki et al. 2014; Baki et al. 2012; Rahman et al. 2013), the state of zero effective stress may be transient during a load cycle where cyclic stress can still be sustained for a few cycles with imposed loading magnitudes or will lead to complete loss of soil strength once triggered. In this paper, pwp generation was examined for soil specimens which manifested cyclic instability. Although numerous studies have been conducted to study pwp generation behaviour of granular soils in the past, it is yet to reach a consensus (Baziar et al. 2011; Belkhatir et al. 2014). Moreover, past relevant studies were mainly concentrated on clean sand (Hazırbaba 2005) although natural as well as artificial (e.g. hydraulic fills) soil deposits often contain considerable amount of fines (particles passing 0.075 mm sieve). Also, the presence of fines in soil matrix has significant influence on generation of excess pwp (Belkhatir et al. 2014). Further, selection of an appropriate density index in describing mechanical behaviours of sand with fines is a challenge (Rahman et al. 2008; Thevanayagam 1998).

[1]Lecturer, Dept. of Civil Eng. & QS, Military Technological College, Muscat, Oman, abdul.baki@mtc.edu.om
[2]Senior Lecturer, School of NBE & Barbara Hardy Institute, UniSA, Australia, mizanur.rahman@unisa.edu.au
[3]Associate Professor, School of Engineering & IT, UNSW, Canberra, Australia, r.lo@adfa.edu.au

Although numerous models have been proposed in the literature to predict the development of excess pwp under cyclic loading for sands (Cetin and Bilge 2012; Chang et al. 2007; Polito et al. 2013), silt (Wijewickreme and Sanin 2010) and silty sand (Hazirbaba and Rathje 2009), limited research work found in the literature where a direct comparison in generation of pwp between tests had been illustrated for silty sands under undrained cyclic triaxial loading. Comparing cyclic triaxial test results at the same void ratio, Erten and Maher (1995) showed that generation of excess pwp increased with the increase in fines content, f_c, up to 30%. Based on cyclic triaxial test results on Chlef sand with fines, Belkhatir et al. (2011) demonstrated that excess pwp generation increases with the increase in f_c up to 40% where comparison was made at a constant relative density of 53%. They kept initial effective confining stress, p'_0, and peak and trough deviatoric stresses (q_{peak} and q_{trough} respectively) same between tests. For cyclic direct simple shear tests results, Hazirbaba and Rathje (2009) showed that the presence of fines decreases excess pwp generation regardless examined index parameters i.e. relative density, sand skeleton void ratio and overall void ratio. Similar finding was reported in Baziar et al. (2011) for a silty sand tested under stress-controlled cyclic hollow torsional tests. Abovementioned literature show contradictory findings regarding effects of f_c on generation of pwp of silty sands, bearing in mind that experiments were performed in different testing devices.

The objectives of this research are to examine (i) the effect of f_c and (ii) applied q_{peak} and q_{trough} on excess pwp generation of a silty sand. Equivalent granular state parameter (see Appendix) is used to synthesis test results.

Experimental Program

For this study, a triaxial testing system with PC-controlled data logging and stress/strain control capabilities was used. Axial load was applied by a force actuator located beneath the cell and a loading ram connected to the bottom platen. However, an internal load cell, located at the top of the specimen, was used to measure the resistance developed by the specimen. A pair of internal linear variable displacement transducer (LVDTs), mounted directly across the top platen, was used to measure axial deformation at the early stage of shearing whereas an external LVDT was used at large deformation. The pore pressure line was connected to a small capacity Digital Pressure Volume Controller (DPVC) which served two purposes: i) controlling back pressure and measurement of volume change in drained stage, and ii) ensuring nil volume change and measuring pwp generation during undrained shearing.

Tests were conducted for sand-fines mixtures which were prepared by mixing Sydney sand (SP) with a well-graded and low-plasticity fines called MII fines herein. MII fines was a mixture of locally available fines from Majura river bank deposits (2/3) and commercial kaolin (1/3). Specific gravity of Sydney sand and uniformity coefficient of MII fines was 2.65 and 21.56 respectively. Grading curves of tested materials is shown in Figure 1. Soil specimens of 100 mm diameter and 100 mm height were prepared by a modified moist tamping method (Bobei et al. 2009; Lo et al. 2010). Saturation was accomplished in two steps: vacuum flashing followed by back pressure saturation to a Skempton's B value > 0.98. Free ends with enlarged platens were used to reduce end restraint to an insignificant level (Lo et al. 1989). The physical properties, soil specimen preparation of the tested materials and testing arrangements had been detailed elsewhere (Baki et al. 2014; Baki et al. 2012; Lo et al. 2010; Rahman and Lo 2012).

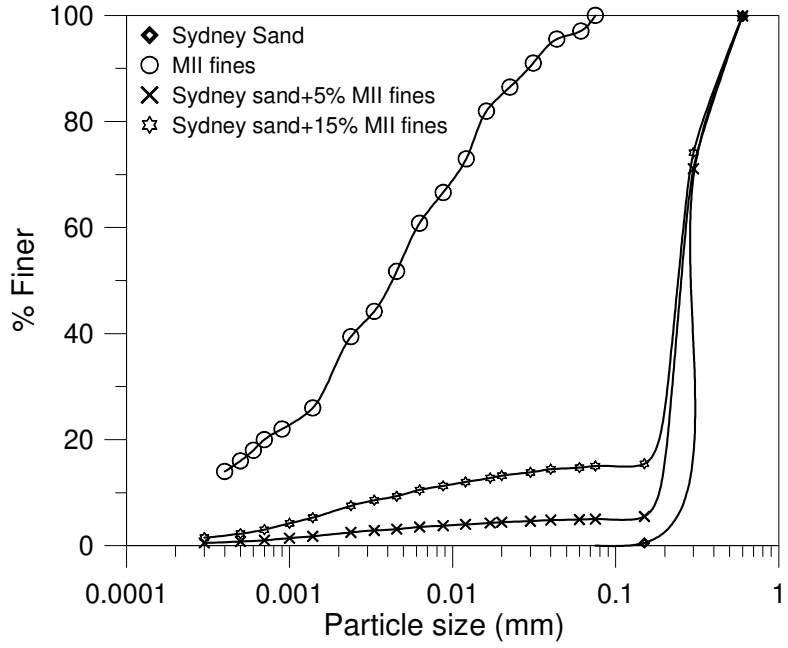

Figure 1. Gradation curves of tested materials

A total of 6 two-way non-symmetrical undrained cyclic triaxial tests, as tabulated in Table 1, have been analysed and discussed here. All the discussed tests were tested at $\psi^* > 0$ and showed cyclic instability behaviour which triggered in the compression side of stress space. Tests were conducted at p'_0 of 600 kPa and covered a range of initial testing conditions of: f_c from 5 to 15%, void ratio prior to shearing, e_0, from 0.675 to 0.810. Test results are compared in pairs where a test pair is defined as having the same $\psi^*(0)$ and stress state both at the start of undrained shearing.

Table 1. Summary of cyclic tests.

Test ID	p'_0 **(kPa)**	e_0	$\psi^*(0)$	q_{peak} **(kPa)**	q_{trough} **(kPa)**	**Comparison**
C-15-57	600	0.654	0.086	183	-83	Effect of e_0
C-05-78	600	0.810	0.089	179	-82	
C-15-97	598	0.650	0.081	185	-94	Effect of q_{peak}
C-05-117	600	0.803	0.083	244	-95	
C-15-71	600	0.678	0.112	151	-63	Effect of q_{trough}
C-15-79	600	0.675	0.109	154	-93	

Results and Analysis

Figure 2 shows pwp generation curves of a test-pair, C-15-57 and C-05-78, with nearly same ψ^* (a difference of 0.003) but had a different f_c (15% and 5% respectively) and e_0 (0.654 and 0.810 respectively). Test results are plotted in normalized form where excess pwp is normalized by p_0'

and number of loading cycle, N, also normalised by $N_{100\%pwp}$ where $N_{100\%pwp}$ is the number of loading cycles at 100% excess pwp generation.

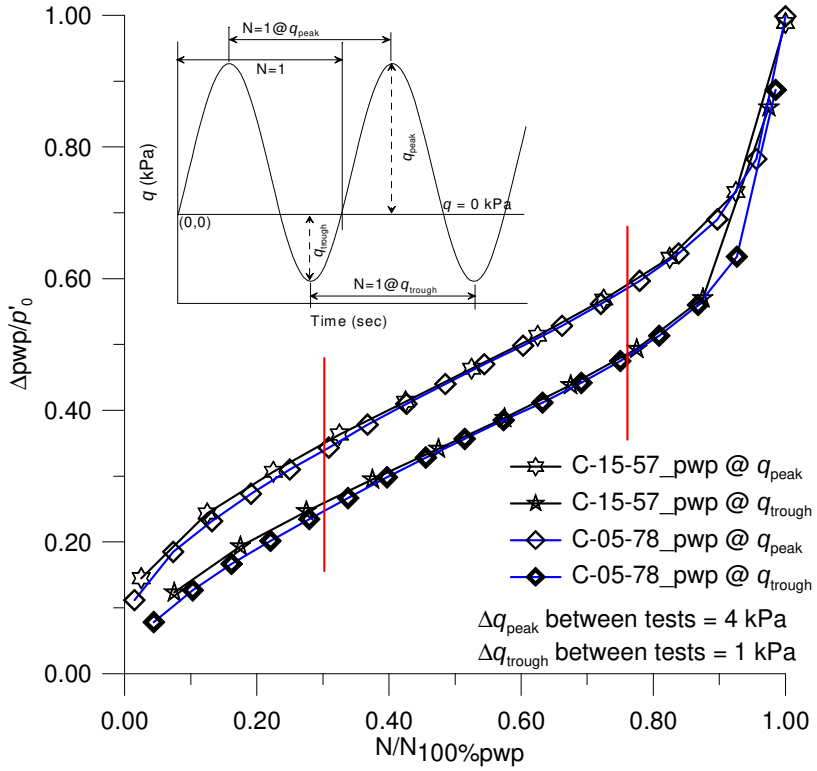

Figure 2. Comparison of pwp generation of a test-pair (C-15-57 & C-05-78) with nearly same ψ^*

As in Figure 2, the excess pwp increased significantly during the first few loading cycles followed by a slower rate with further application of loading. In the first loading cycle, developed excess pwp for C-15-57 was about 16% whereas it was about 12% for C-05-78. For both tests, excess pwp increased at a greater rate per loading cycle upto $N/N_{100\%pwp} = 0.30$ (marked by a vertical thick line in Figure 2). Thereafter, the slope of excess pwp remained almost constant upto $N/N_{100\%pwp} \approx 0.80$ (marked by a second vertical thick line in Figure 2) where a progressive increase in excess pwp occurred with increasing number of loading cycles. Thereafter, in the last few loading cycles, a dramatic shoot-up of excess pwp was observed. To better evaluate the history of excess pwp in relation to the accumulation of deviatoric strain, ε_q, $N/N_{100\%pwp}$ vs ε_q (%) response has been plotted in Figure 3 for this comparison only. Figure 3 (zoomed) in correspondence with Figure 2 shows that, at ε_q of 0.73%, 75% excess pwp developed for C-15-57 whereas it was 80% for C-05-78. Thereafter, the slope of both excess pwp curves started to increase and a dramatic change in both excess pwp and ε_q was observed in the last 2-3 loading cycles (Figure 3). At this state, soil specimen started to loose its strength and cyclic instability triggered followed by complete loss of soil strength within 2-3 loading cycles. For this illustrated test pair, excess pwp curves superimposed each other despite having different e_0 and f_c. Thus, it appears that ψ^* may serve as an index parameter for analysis of excess pwp generation irrespective of f_c.

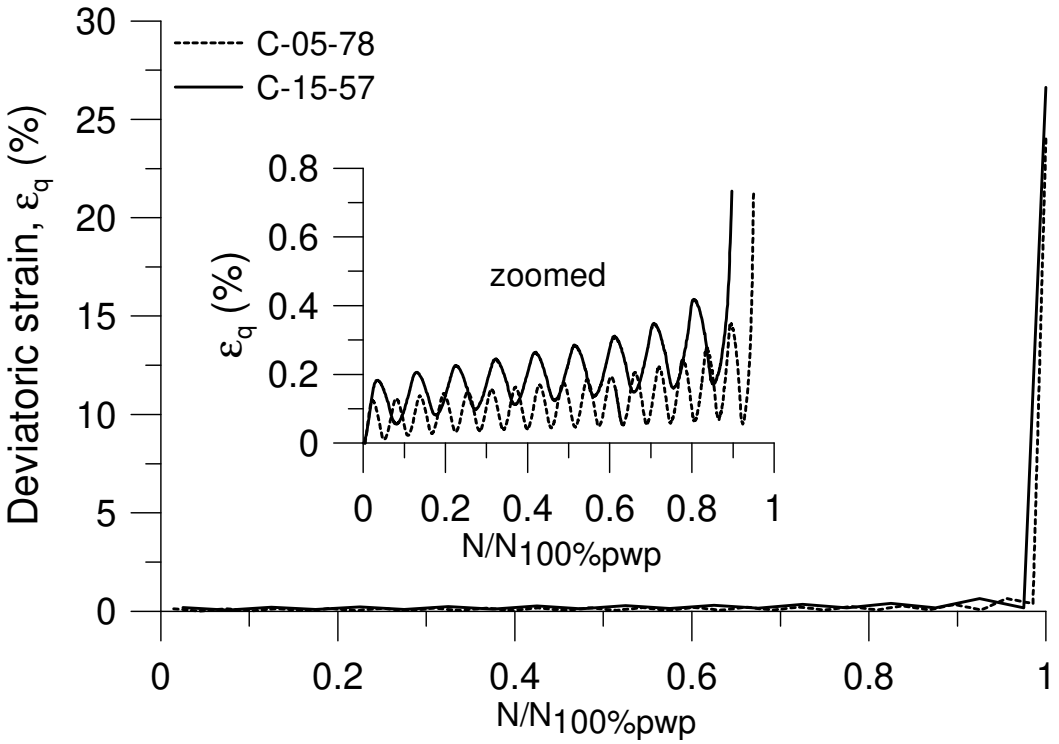

Figure 3. Deviatoric strain, ε_q vs $N/N_{100\%pwp}$ response of test-pair C-15-57 & C-05-78

Excess pwp generation curves of another test pair, C-15-97 and C-05-117, with nearly same ψ^* (a difference of 0.002), are presented in Figure 4. Same q_{trough} was applied for both tests. However, test C-05-117 was tested at a higher q_{peak} of 59 kPa than C-15-97. Thus, this comparison will give opportunity to examine how a higher magnitude of q_{peak} influences in excess pwp generation. Likewise previous illustration, this test pair also showed similar trend in excess pwp generation: accelerated excess pwp generation in the first few loading cycles followed by a constant rate of change before abrupt development of excess pwp in the last few loading cycles (Figure 4). Specimen C-15-97 reached 94% excess pwp in 5 loading cycles whereas it took 9 loading cycles for C-05-117 to develop 98% excess pwp. Except last few (N≈3) loading cycles, the gap between excess pwp generation curves was not considerably significant (Figure 4). Also the shape of the curves was similar. Thus, examined test results suggest minimal effect of q_{peak} in generation of excess pwp.

To examine the role of different q_{trough} on generation of excess pwp between tests, results of C-15-71 and C-15-79 have been plotted in Figure 5. Although both tests had same ψ^*, q_{peak} and p'_0, test C-15-79 had a higher magnitude (differ by 30 kPa) of q_{trough} than C-15-71. As in Figure 5, a noticeable difference between the excess pwp curves was observed. A faster excess pwp development occurred for C-15-79 than C-15-71. Although the shape of the curves between $N/N_{100\%pwp}$ values of 0.40 and 0.80 was similar, the gap between curves was evident. The number of loading cycles required to cause 100% pwp for C-15-71 was 36 whereas C-15-79 reached 100% pwp only in 13 loading cycles. This indicates the vulnerability of a higher magnitude of q_{trough} in excess pwp generation. This can be explained by the fact of having less magnitude of the slope of instability zone in extension side than that of compression side of the stress space.

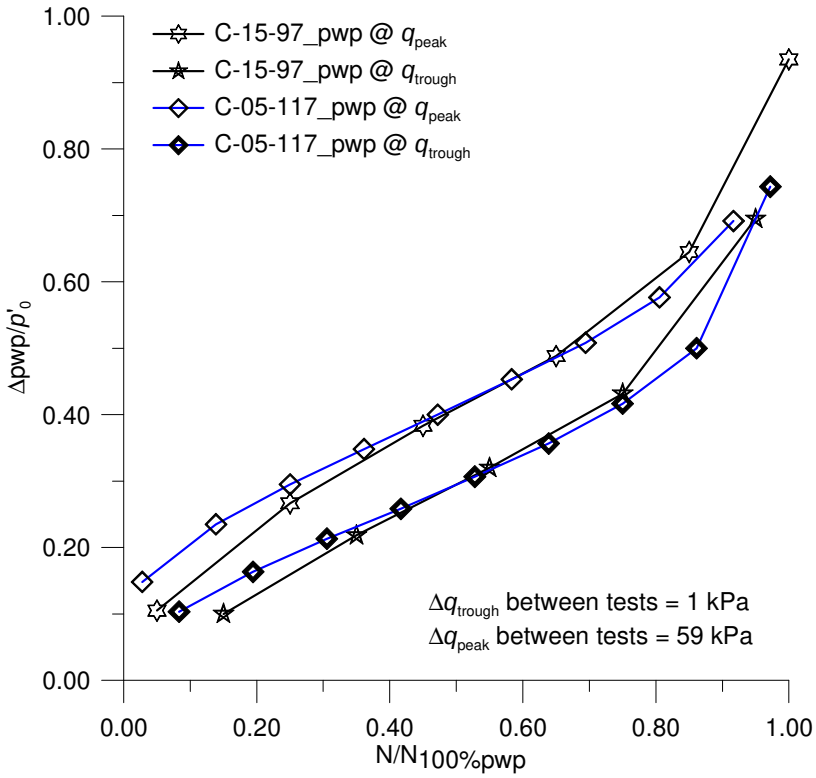

Figure 4. Excess pwp generation of tests C-15-97 & C-05-117 [same q_{trough} but different q_{peak}]

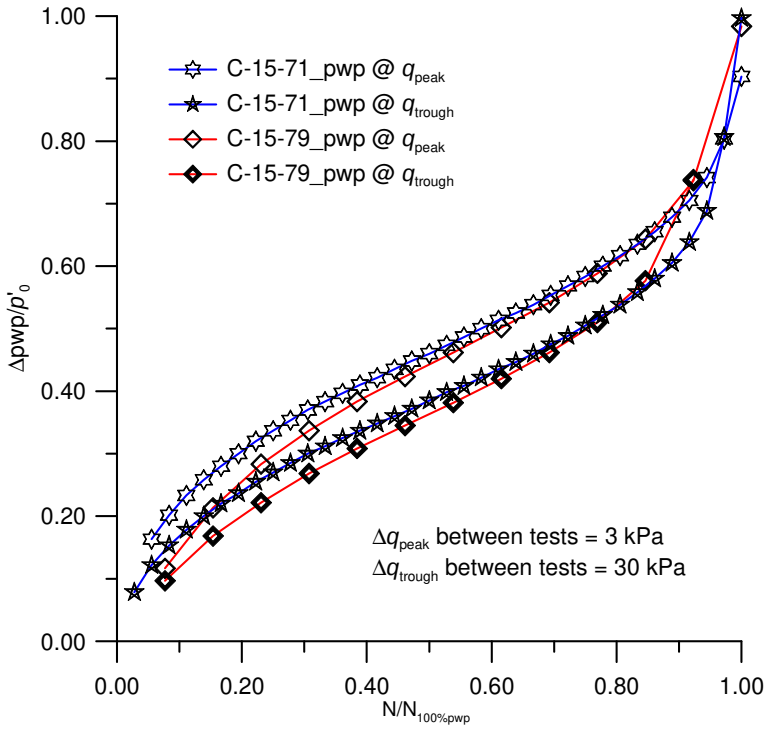

Figure 5. Excess pwp generation of tests C-15-71 & C-15-79 [same q_{peak} but different q_{trough}]

Conclusions

The effect of fines, imposed peak and trough deviatoric stresses on generation of excess pore water pressure of Sydney sand with fines (up to 15%) had been examined under two-way non-symmetrical undrained cyclic triaxial loading. Tests were compared in pairs and equivalent granular state parameter was used to synthesis test results. All the examined tests showed cyclic instability and triggered in the compression side of stress space. Analysed test results indicate that, as long as other applied initial testing parameters kept same between the tests, equivalent granular state parameter can be used effectively as an index parameter in comparing excess pore water pressure generation of silty sand irrespective of fines content (up to a threshold fines content). It was also appeared for compared test pairs that q_{trough} has more detrimental effect compared to q_{peak} in excess pore water pressure generation of tested silty sand. It is to be noted that the concept of equivalent granular state parameter is applicable up to a threshold fines content of a given soil matrix. For tested soil, threshold fines content was 40%.

Acknowledgments

The first author gratefully acknowledges the support received under University College Postgraduate Research Scholarship from The University of New South Wales (UNSW), Canberra, Australia while conducted research presented herein.

References

Baki, M.A.L., Rahman, M.M., and Lo, S.R. Predicting onset of cyclic instability of loose sand with fines using instability curves. *Soil Dynamics and Earthquake Engineering*, 2014; **61-62**: 140-151.

Baki, M.A.L., Rahman, M.M., Lo, S.R., and Gnanendran, C.T. Linkage between static and cyclic liquefaction of loose sand with a range of fines contents. *Canadian Geotechnical Journal*, 2012; **49**(8): 891-906.

Baziar, M.H., Shahnazari, H., and Sharafi, H. A laboratory study on the pore pressure generation model for Firouzkooh silty sands using hollow torsional test. *International Journal of Civil Engineering,* 2011; **9**(2): 127-134.

Belkhatir, M., Schanz, T., Arab, A., and Della, N. Experimental Study on the Pore Water Pressure Generation Characteristics of Saturated Silty Sands. Arabian *Journal for Science and Engineering*, 2014; **39**(8): 6055-6067.

Belkhatir, M., Arab, A., Schanz, T., Missoum, H., and Della, N. Laboratory study on the liquefaction resistance of sand-silt mixtures: effect of grading characteristics. *Granular Matter,* 2011; **13**(5): 599-609.

Bobei, D., Lo, S.R., Wanatowski, D., Gnanendran, C.T., and Rahman, M.M. A modified state parameter for characterizing static liquefaction of sand with fines. *Canadian Geotechnical Journal*, 2009; **46**(3): 281-295.

Cetin, K.O., and Bilge, H.T. Cyclic Large Strain and Induced Pore Pressure Models for Saturated Clean Sands. *Journal of Geotechnical and Geoenvironmental Engineering*, 2012; **138**(3): 309–323.

Chang, W.-J., Rathje, E.M., II, K.H.S., and Hazirbaba, K. In Situ Pore-Pressure Generation Behavior of Liquefiable Sand. *Journal of Geotechnical and Geoenvironmental Engineering*, 2007; **133**(8): 921-931.

Charlie, W.A., Bretz, T.E., Schure, L.A., and Doehring, D.O. Blast-Induced Pore Pressure and Liquefaction of Saturated Sand. *Journal of Geotechnical and Geoenvironmental Engineering*, 2013; **139**(8): 1308-1319.

Erten, D., and Maher, M.H. Cyclic Undrained Behavior of Silty Sand. *Soil Dynamics and Earthquake Engineering*, 1995; **14**(2): 115-123.

Hazirbaba, K., and Rathje, E.M. Pore Pressure Generation of Silty Sands due to Induced Cyclic Shear Strains. *Journal of Geotechnical and Geoenvironmental Engineering*, 2009; **135**(12): 1892-1905.

Hazırbaba, K. *Pore Pressure Generation Characteristics of Sands and Silty Sands: A Strain Approach*. PhD Thesis, University of Texas at Austin, 2005.

Lo, S.R., Chu, J., and Lee, I.K. A Technique for reducing membrane penetration and bedding errors. *Geotechnical Testing Journal*, 1989; **12**(4): 311-316.

Lo, S.R., Rahman, M.M., and Bobei, D.C. Limited flow characteristics of sand with fines under cyclic loading. *Geomechanics and Geoengineering*, 2010; **5**(1): 15-25.

Polito, C., Green, R.A., Dillon, E., and Sohn, C. Effect of load shape on relationship between dissipated energy and residual excess pore pressure generation in cyclic triaxial tests. *Canadian Geotechnical Journal*, 2013; **50**(11): 1118–1128.

Rahman, M.M., and Lo, S.R. The prediction of equivalent granular steady state line of loose sand with fines. *Geomechanics and Geoengineering*, 2008; **3**(3): 179 - 190.

Rahman, M.M., and Lo, S.R. Predicting the onset of static liquefaction of loose sand with fines. *Journal of Geotechnical and Geoenvironmental Engineering*, 2012; **138**(8): 1037-1041.

Rahman, M.M., Lo, S.R., and Gnanendran, C.T. On equivalent granular void ratio and steady state behaviour of loose sand with fines. *Canadian Geotechnical Journal*, 2008, **45**(10): 1439-1456.

Rahman, M.M., Lo, S.R., and Gnanendran, C.T. Reply to discussion by Wanatowski, D. and Chu, J. on- On equivalent granular void ratio and steady state behaviour of loose sand with fines. *Canadian Geotechnical Journal*, 2009; **46**(4): 483-486.

Rahman, M.M., Baki, M.A.L., and Lo, S.R. Prediction of undrained monotonic and cyclic liquefaction behaviour of sand with fines based on equivalent granular state parameter. *International Journal of Geomechanics*, ASCE, 2014; **14**(2):254-266.

Thevanayagam, S. Effect of fines and confining stress on undrained shear strength of silty sands. *Journal of Geotechnical and Geoenvironmental Engineering*, 1998; **124**(6): 479-491.

Thevanayagam, S., Shenthan, T., Mohan, S., and Liang, J. Undrained fragility of clean sands, silty sands, and sandy silts. *Journal of Geotechnical and Geoenvironmental Engineering*, 2002; **128**(10): 849-859.

Wijewickreme, D., and Sanin, M.V. Post-cyclic Reconsolidation Strains in Low-plastic Fraser River Silt due to Dissipation of Excess Pore Water Pressures. *Journal of Geotechnical and Geoenvironmental Engineering*, 2010; **136**(10): 1347-1357.

Xenaki, V.C., and Athanasopoulos, G.A. Liquefaction resistance of sand–silt mixtures: an experimental investigation of the effect of fines. *Soil Dynamics and Earthquake Engineering*, 2003; **23**: 183-194.

Appendix

To take into account the presence of fines on density state, one can define an equivalent granular void ratio, e^*, as an alternative to e, as proposed by Thevanayagam et al. (2002)

$$e^* = \frac{e + (1-b) f_c}{1 - (1-b) f_c} \tag{1}$$

where f_c is fines content and b represents the fraction of fines that are active in force transmission in the soil skeleton. Eqn (1) above requires f_c is less than a threshold value f_{thre}, so that the soil fabric is still of a fines-in-sand matrix. To predict b, Rahman and Lo (2008) proposed a semi-empirical equation expressed as below.

$$b = \left[1 - \exp\left(-0.3\frac{(f_c / f_{thre})}{k}\right)\right] \times \left(r\frac{f_c}{f_{thre}}\right)^r \quad (2)$$

where r = d/D, $k = 1 - r^{0.25}$, and where D is the size of sand and d is the size of fines. Since sand and fines are generally not single-size materials, D/d was generalized to D_{10}/d_{50}, where the subscripts denote fractile passing. As an initial approximation, f_{thre} can be taken as 0.30; but it may be determined more reliably using the following equation developed by Rahman et al. (2009).

$$f_{thre} = 0.40\left(\frac{1}{1+e^{\alpha-\beta\chi}} + \frac{1}{\chi}\right) \quad (3)$$

Where $\alpha = 0.50$ and $\beta = 0.13$.

The critical state (or steady state) data points, when plotted in a e^*-log(p') space, follows a single relationship irrespective of f_c. This single relationship is referred to as the equivalent granular steady state line (EG-SSL). ψ^* is defined as the distance (measured in e^* direction) between the state point from the EG-SSL (Rahman et al. 2008) as illustrated in Figure 6 below.

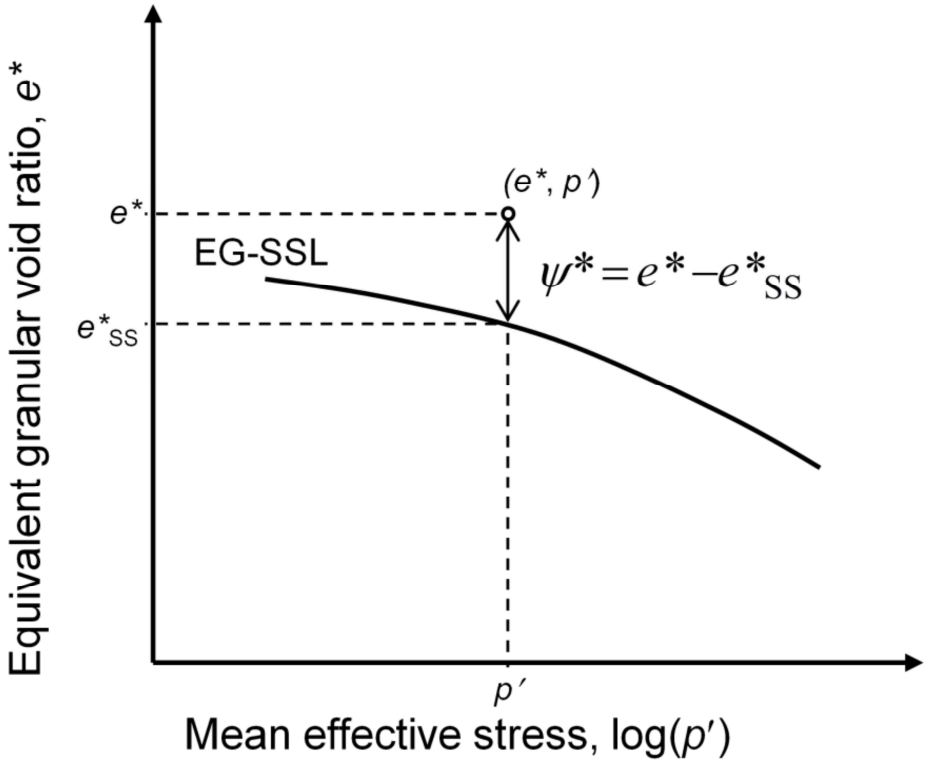

Figure 6. Definition of ψ^*